HHS Public Access

Author manuscript

*Microvasc Res*. Author manuscript; available in PMC 2017 February 18.

Published in final edited form as:

*Microvasc Res*. 2010 July ; 80(1): 133–141. doi:10.1016/j.mvr.2010.02.006.

# Role of endothelial cell-selective adhesion molecule in hematogeneous metastasis

**Husni M. Cangara**[a,b,d], **Tatsuro Ishida**[b,*], **Tetsuya Hara**[b], **Li Sun**[b], **Ryuji Toh**[b], **Yoshiyuki Rikitake**[b], **Ramendra K. Kundu**[c], **Thomas Quertermous**[c], **Ken-ichi Hirata**[b], and **Yoshitake Hayashi**[a]

[a] Division of Molecular Medicine and Genetics, Department of Pathology, Kobe University Graduate School of Medicine, Kobe, Japan

[b] Division of Cardiovascular Medicine, Department of Internal Medicine, Kobe University Graduate School of Medicine, 7-5-1 Kusunoki-cho, Chuo-ku, Kobe 650-0017, Japan

[c] Division of Cardiovascular Medicine, Stanford University School of Medicine, Stanford, CA, USA

[d] Department of Pathology, Medical Faculty of Hasanuddin University, Makassar, Indonesia

## Abstract

The spread of malignant cells from a localized tumor is thought to be directly related to the number of microvessels in the tumor. The endothelial cell-selective adhesion molecule (ESAM) is a member of the immunoglobulin superfamily that mediates homophilic interactions between endothelial cells. Previous studies have indicated that ESAM regulates angiogenesis in the primary tumor growth and endothelial permeability. In this study, we aimed to further elucidate the role of ESAM in tumor metastasis through angiogenic processes. ESAM expression was higher in hypervascular metastatic tumor tissues than in normal tissues in human lungs. Cell culture studies found that conditioned medium from B16F10 melanoma cells increased ESAM expression in endothelial cells and promoted endothelial migration and tube formation. The B16F10 medium-induced endothelial migration and tube formation were significantly attenuated when *ESAM* was downregulated by siRNA transfection. Intravenous injection of B16F10 cells into *ESAM*+/+ and *ESAM*−/− mice for comparison of metastatic potential resulted in the number of metastatic lung nodules in *ESAM*−/− mice being 83% lower than of those in *ESAM*+/+ mice. The microvascular density in the tumor was also lower in *ESAM*−/− than in *ESAM*+/+ mice. These findings indicate that ESAM regulates tumor metastasis through endothelial cell migration and tube formation in metastatic nodules. Inhibition of ESAM may therefore inhibit tumor metastasis by inhibiting the angiogenic processes.

### Keywords

Angiogenesis; Adhesion molecule; Metastasis; Endothelial cells; Tumor

* Corresponding author. Fax: +81 78 382 5859. ishida@med.kobe-u.ac.jp (T. Ishida).

## Introduction

Angiogenesis is a phenomenon in which new capillaries are generated by sprouting or splitting from pre-existing vessels (Risau, 1997; Carmeliet and Jain, 2000). The process of angiogenesis involves endothelial cell activation and degradation of extracellular matrix and basal membrane, which is followed by endothelial cell migration, proliferation, and subsequent differentiation into functional blood vessels (Bendeck, 2004). Under normal conditions, angiogenesis occurs during wound healing, female reproduction, embryonic development, organ formation, tissue regeneration and remodeling (Ferrara and Kerbel, 2005). Unregulated angiogenesis, on the other hand, is observed under pathologic conditions such as tumor growth, diabetic retinopathy, and inflammation (Coultas et al., 2005). In particular, the development of blood vessels is an essential step in the growth of primary tumors. Moreover, it is believed that angiogenesis is not only a prerequisite for tumor growth but also a major factor affecting the invasion and metastatic spread of malignant cells (Sökmen et al., 2001; Folkman, 1995).

Interaction between tumor cells and vascular endothelium is important for cancer metastases and depends on the function of interendothelial junctions (Dejana et al., 2000; Vestweber, 2000; Miles et al., 2008). The endothelial cell-selective adhesion molecule (ESAM) is a new member of the immunoglobulin superfamily (Hirata et al., 2001), which is found at interendothelial cell contacts. ESAM is co-localized with tight junction proteins and mediates homophilic interactions between endothelial cells (Hirata et al., 2001; Nasdala et al., 2002). Previous studies have demonstrated that ESAM plays a role in the growth of primary tumor in mice, since targeted deletion of *ESAM* resulted in attenuation of tumor angiogenesis and tumor growth (Ishida et al., 2003). On the other hand, ESAM has been shown to regulate endothelial permeability and leukocyte transmigration (Wegmann et al., 2006; Hara et al., 2009), which suggests that deletion of *ESAM* may modulate trans-endothelial migration of tumor cells into the tissue. It therefore remains to be elucidated if *ESAM* deficiency can attenuate or promote tumor metastasis. In this study, we employed a murine model of tumor metastasis and compared the hematogeneous metastasis between *ESAM*-deficient mice (*ESAM*−/−) (Ishida et al., 2003) and control *ESAM*+/+ mice. In addition, we characterized the expression of ESAM in human metastatic tumors and further explored the effects of *ESAM* downregulation on *in vitro* angiogenic processes.

## Materials and methods

### Cell culture

B16F10 melanoma, Chinese Hamster Ovary (CHO), L-fibroblast (LF), and Lewis Lung Carcinoma (LLC) were obtained from American Type Culture Collection (Manassas, VA). EA.hy926, a human endothelial cell line, was kindly provided by Dr. C. J. Edgell (University of North Carolina, Chapel Hill, NC). The cells were maintained in DMEM supplemented with 10% fetal bovine serum and penicillin and streptomycin (all from Sigma-Aldrich, St. Louis, MO).

### Murine model of pulmonary hematogeneous metastasis

All animal experiments were conducted at the Kobe University Graduate School of Medicine in accordance with the Institutional Guidelines for Animal Experiments. B16F10 cells, which do not express ESAM, were injected ($1\times10^6$ cells) into the tail veins of *ESAM* +/+ and *ESAM*−/− mice (Ishida et al., 2003). Three weeks later, the mice were sacrificed and their lungs excised. The number of metastatic nodules in the whole lung was counted macroscopically. For histological analyses, the lungs were fixed with 10% paraformaldehyde, embedded in paraffin, sliced into 8-μm sections, and then stained with hematoxylin and eosin (H&E). Diameter of the metastatic nodules was determined by averaging the diameters of 100 randomly selected nodules in each lung with the aid of Image-J software, an open-source Java-based image analysis program developed at the National Institutes of Health (Bethesda, MD).

### Histological characterization of mouse and human tumors

For immunofluorescence, tumor sections were incubated with the anti-mouse CD31 antibody (BD Pharmigen, San Diego, CA) and then with FITC-conjugated anti-rat IgG antibody (Sigma-Aldrich) as a secondary antibody. Sections were counter-stained with DAPI antifade (Chemicon, Temecula, CA) and mounted with a fluorescent mounting medium (DAKO, Carpinteria, CA). The vascular structure was identified under confocal microscopy (× 200) in 50 random fields in each tumor section. Tumor angiogenesis and vascular morphologies were scored as functional vessel density, number of branch points per vessel, number of lumens formed, and length of vessels (Gupta et al., 2007).

Paraffin-embedded sections of human normal and tumor tissues were obtained from Dr. Y. Maniwa (Division of Thoracic Surgery, Kobe University) and Dr. Y. Imai (Kobe City Medical Center General Hospital) with informed consent from the patients. The clinical study was approved by the Institutional Review Board of Kobe University Graduate School of Medicine. Western blotting and immunohistochemistry were performed using anti-ESAM antibodies (R&D System, Minneapolis, MN), or anti-human CD31 antibody (DAKO) as described elsewhere (Orrington-Myers et al., 2006; Yoder et al., 2007). Counterstaining was performed with hematoxylin.

### Terminal nucleotidyl transferase-mediated nick end labeling (TUNEL) assay

The TUNEL assay was performed with an *in situ* apoptosis detection kit (Takara, Tokyo, Japan). The number of apoptotic cells was evaluated by counting the number of TUNEL-positive cells in 50 random fields of the metastatic nodule under a fluorescence microscope.

### Cell stimulation assays

LLC or B16F10 cells were grown on 6-cm culture plates until subconfluency. After washing with phosphate-buffered saline (PBS), the cells were incubated in serum-free DMEM for 24 h. The culture supernatant was then collected, centrifuged, and used as the cancer medium. Culture supernatants of LF and CHO cells were used as non-cancer media. Because primary endothelial cells were not suitable for long-time incubation without serum, endothelial EA.hy926 cells were cultured and stimulated with the cancer medium, a non-cancer medium, or serum-free DMEM alone (control medium) for 24 h. The cells were then lysed

and equal amounts of whole cell proteins were subjected to western blotting for ESAM expression.

The siRNA-mediated knockdown of *ESAM* was performed using a siGENOME SMARTpool specific for human *ESAM* (Dharmacon, Lafayette, CO). The EA.hy926 cells was transfected with the *ESAM* siRNA or stealth RNAi negative control by using a Lipofectamine RNAiMAX reagent (Invitrogen, Carlsbad, CA). The cells were used 24–48 h after the transfection for subsequent experiments.

### In vitro migration assays

The endothelial wound healing assay was performed as described with some modifications (Herard et al., 1996). Confluent EA.hy926 cells cultured on six-well plates were transfected with control- or *ESAM*-siRNA and then incubated for 24 h. The endothelial wound was created by scraping the monolayer with a narrow pipette tip. After washing with PBS, 4 mL conditioned medium of B16F10 cells or serum-free medium was added to the well. Cells were stained with 0.5% crystal violet, and the extent of cell migration was assessed by counting the number of cells that had migrated into a clear area (10 random fields/well) 0, 6, and 10 h after scraping.

### Proliferation, apoptosis, and tube formation assays

The endothelial proliferation assay was performed as described with some modifications (Adams et al., 2005). Briefly, EA.hy926 cells were transfected with control- or *ESAM*-siRNA. Two hours later, the culture medium was replaced with control or B16F10 medium and incubated for 3 days. Cell proliferation was measured with the WST-1 assay (Roche Applied Science, Basel, Switzerland).

For the apoptosis assay (Takatani et al., 2004), EA.hy926 cells were transfected with control- or *ESAM*-siRNA and then incubated with control or B16F10 medium for 3 days. The cells were stained with Hoechst 33258 (Dojindo, Kumamoto, Japan). The average number of apoptotic nuclei was calculated under a fluorescence microscope by counting the number of condensed, fragmented nuclei in 20 random microscopic fields.

For the tube formation assay, EA.hy926 cells were plated onto Matrigel-coated (BD Biosciences, Bedford, MA) plates (Gho et al., 1999), and transfected with control- or *ESAM*-siRNA. The cells were then incubated with control or B16F10 medium for 16 h.

### Statistical analysis

Statistical significance was determined by one-way analysis of variance (ANOVA) with the *t*-test (unpaired). Data were expressed as mean±SEM and differences were considered significant at $P<0.05$.

## Results

### ESAM is increased in the vascular endothelium of metastatic lung tumors in humans

To investigate the expression of ESAM in human metastatic tumors, we characterized ESAM localization in normal lung and metastatic tumor tissues. ESAM expression in metastatic tumor tissues of malignant melanoma, leiomyosarcoma, and squamous carcinoma was compared with that in the normal lung tissue. Immunohistochemical analysis showed ESAM expression along the endothelium of blood vessels in these tumors and co-localization with the endothelial marker CD31 (Fig. 1A). Western blotting disclosed that the ESAM protein level was significantly higher in metastatic adenocarcinoma of the lung than in normal lung tissue (Fig. 1B). These findings suggest that ESAM expression is increased in the metastatic tumor tissue.

### Cancer cells induce ESAM expression

To determine whether upregulation of ESAM in hypervascular tumor tissues merely reflect the increased vascular density or ESAM is selectively upregulated in the tumor vasculature, we investigated the role of tumor cells on endothelial ESAM expression. Because primary endothelial cells were not suitable for long-term culture without serum and endothelial cell growth factors, we used endothelial EA. hy926 hybrid cells. We harvested culture medium of cancer cell lines including B16F10 or LLC, and stimulated EA.hy926 cells with cancer medium. Western blotting showed a marked induction of ESAM in EA. hy926 cells exposed to either B16F10 or LLC medium, while a non-cancer (CHO or LF) or control medium did not affect ESAM levels (Fig. 2A). This finding suggests that cancer cells may secrete some factor(s) that induce ESAM expression in endothelial cells.

### Endothelial migration was selectively reduced by downregulation of ESAM

To further investigate the role of ESAM expression in endothelial cell activity, we reduced the level of *ESAM* in EA.hy926 cells by means of siRNA targeted against *ESAM*, while non-targeting siRNA was used as control. We confirmed that transfection of siRNA against *ESAM* resulted in a marked reduction in ESAM protein expression (Fig. 2B).

We next used these transfected cells to perform an *in vitro* tube formation assay. In the presence of the B16F10 medium, control EA.hy926 cells formed an organized, elongated tube-like structure resembling capillaries with an extensive network, while the formation of the tubular structure was attenuated when the control medium was used (Fig. 2C). In contrast, when *ESAM* was downregulated, the tube-like structure was barely induced. These findings suggest that ESAM expression in endothelial cells is associated with the cancer medium-induced capillary formation.

Formation of tube-like structures consists of several processes including endothelial migration, proliferation, and apoptosis. We therefore performed *in vitro* migration assays using these control or *ESAM*-downregulated EA.hy926 cells. The B16F10 medium induced migration of control EA.hy926 cells to a greater extent than did the control medium (Fig. 3). In contrast, when *ESAM* was downregulated, cells hardly migrated in response to either the control or B16F10 medium. On the other hand, we found no difference in cell proliferation

or apoptosis between *ESAM*- and control-siRNA transfected EA.hy926 cells in response to either control or B16F10 medium (data not shown). These findings suggest that ESAM expression selectively modulates endothelial migration in response to cancer medium.

### ESAM deficiency attenuates lung metastasis of melanoma cells

To determine if ESAM modulates tumor metastasis, we employed a murine model of experimental hematogeneous metastasis using *ESAM*−/− mice. B16F10 melanoma cells were injected into the tail vein of *ESAM*+/+ and *ESAM*−/− mice, and assessment of hematogeneous metastasis in the lung showed that the number of metastatic nodules was significantly lower in *ESAM*−/− than in *ESAM*+/+ mice (Fig. 4A). We confirmed that ESAM was not detected in the lung of *ESAM*−/− mice (Fig. 4A, bottom, right). Moreover, metastatic nodules in *ESAM*−/− mice were smaller in size than those in *ESAM*+/+ mice (Fig. 4B). Histological analysis revealed that the metastatic nodules in both mouse groups exhibited similar typical characteristics of melanoma such as melanin pigments (Fig. 4B, high magnification).

### ESAM deficiency results in reduced angiogenesis and enhanced apoptosis in metastasis

Because ESAM is known to be involved in tumor angiogenesis in primary tumors, we analyzed vascular density in the metastatic nodule by means of anti-CD31 staining. Angiogenesis can be expressed as the number of blood vessels in metastatic nodules, and abundant blood vessels were observed in *ESAM*+/+ mice, while the number was significantly reduced in *ESAM*−/− mice (Figs. 5A and B). Closer examination revealed that blood vessels in *ESAM*−/− mice displayed some morphological changes: the tumor blood vessels were shorter and had fewer lumens and fewer branch points compared to those of *ESAM*+/+ mice (Figs. 5A and B). These findings suggest that targeted inactivation of *ESAM* resulted in a reduction in angiogenesis not only in the primary but also in the metastatic tumors.

It has been suggested that inhibition of angiogenesis induces apoptosis of adjacent tumor cells, and as a result may inhibit tumor growth and cause tumor regression (Brooks et al., 1994). We therefore employed the TUNEL assay to compare the number of apoptotic cells in the metastatic nodules between the mouse groups (Fig. 6). There were more apoptotic cells in *ESAM*−/− mice than in *ESAM*+/+ mice, which suggests that the diminished angiogenesis in the metastatic nodules probably forced the tumor cells into apoptosis.

## Discussion

Angiogenesis consists of several processes including endothelial cell activation, proliferation, migration, tube formation and capillary sprouting (Carmeliet and Jain, 2000). It has been postulated that angiogenesis is essential not only for primary tumor growth but also for metastasis in animal models and in humans (Kerbel, 2008; Folkman, 1995; Mihich and Croce, 1999). In fact, some angiogenesis inhibitors have been shown to suppress tumor growth and to introduce tumor dormancy (Brown et al., 2008; Iñiguez et al., 2003).

The present study has shown that ESAM expression is increased in metastatic tumor tissues compared to that in normal tissues in humans. Similarly, previous studies have indicated that

ESAM expression is increased in lymphatic endothelial cells in squamous cell and colorectal carcinomas, and associated with the lymph node metastasis (Clasper et al. 2008). Considering that cancer cells produce and release a number of angiogenic factors (Talks and Harris, 2000), our findings suggest that cancer cells may release unidentified growth factors which induce the expression of ESAM in endothelial cells.

The question will be raised that the increase of the ESAM level is a cause or consequence of the hypervascularity of the tumor. We previously demonstrated that *ESAM* deficiency attenuates the growth of primary tumors by inhibition of neovessel formation (Ishida et al., 2003). The findings of the present study have furthered understanding of the effect of *ESAM* deficiency on blood vessel morphology in metastatic tumor tissues. The absence of *ESAM* was found to be associated not only with a reduction in the number of tumor vessels but also in blood vessel morphology and apoptosis of adjacent tumor cells. These findings suggest that ESAM may modulate the growth of metastatic and primary tumors mainly both by promoting tumor angiogenesis.

Furthermore, the present study has demonstrated that cancer medium-induced endothelial migration was selectively inhibited when *ESAM* expression was downregulated. Thus, ESAM appears to play a pivotal role in the endothelial cell–cell association that is required for the endothelial migration and tubular formation in the presence of metastatic tumors. In this context, ESAM may display functions besides its action on cell-to-cell adhesion. For instance, ESAM may interact with some extracellular matrix protein to cause traction between the cell and matrix. Moreover, ESAM may regulate cytoskeleton organization and cell motility through the interaction with intracellular molecules such as MAGI-1 (Wegmann et al., 2004; Kimura et al., 2010). Further studies are required to elucidate the mechanisms underlying the action of ESAM in endothelial migration.

In the present study, apoptosis of metastatic tumor cells was increased in *ESAM*−/− mice, while endothelial apoptosis or proliferation was not affected by *ESAM* downregulation both *in vivo* and *in vitro*. Given that endothelial migration is selectively regulated by ESAM, we speculate that the tumor cell apoptosis occurred as a consequence of the insufficient blood supply caused by the reduced vascularization in the tumor. Taken together, the attenuated tumor metastasis in *ESAM*−/− mice was most likely attributable to the reduced angiogenesis in the metastatic lesion. Thus, the findings presented here imply that the ESAM would be not only a marker for the tumor vascular density but also a modulator of tumor metastasis and growth.

On the other hand, recent studies have demonstrated that ESAM may regulate endothelial permeability and transendothelial migration of leukocytes (Wegmann et al., 2006; Hara et al., 2009). In this context, it could be hypothesized that *ESAM* deficiency might loosen endothelial mechanical contacts and thereby promote transendothelial migration of tumor cells. The role of ESAM in the transendothelial migration of tumor cells should to be determined in the future.

To summarize, ESAM expression was increased in human metastatic tumor tissues. Tumor cells appear to induce the expression of ESAM, which promotes the endothelial angiogenic

processes in the tumor tissues. Furthermore, we have managed to identify the role of ESAM in tumor angiogenesis and metastasis by using a murine model of hematogeneous metastatis in the lung. Further mechanistic approaches would strengthen the results of this study. However, the findings of our study have thus provided a novel insight into the pathogenesis of tumor angiogenesis and indicate that ESAM could well be a candidate molecule for antiangiogenic therapeutic strategy for malignant tumors.

## Acknowledgments

This work was supported in part by Japan Foundation of Cardiovascular Research and by grants-in-aid for Scientific Research (B)17390103, (C)18659097, and (C) 17590734 from the Ministry of Education, Culture, Sports, Science and Technology (MEXT), Japan.

## References

Adams RL, Adams IP, Lindow SW, Atkin SL. Somatostatin receptors 2 and 5 are preferentially expressed in proliferating endothelium. Br. J. Cancer. 2005; 92:1493–1498. [PubMed: 15812556]

Bendeck MP. Macrophage matrix metalloproteinase-9 regulates angiogenesis in ischemic muscle. Circ. Res. 2004; 94:138–139. [PubMed: 14764648]

Brooks PC, Montgomery AM, Rosenfeld M, Reisfeld MA, Hu T, Klier G, Cheresh DA. Integrin alpha v beta 3 antagonists promote tumor regression by inducing apoptosis of angiogenic blood vessels. Cell. 1994; 79:1157–1164. [PubMed: 7528107]

Brown AP, Citrin DE, Camphausen KA. Clinical biomarkers of angiogenesis inhibition. Cancer Metastasis Rev. 2008; 27:415–434. [PubMed: 18414993]

Carmeliet P, Jain RK. Angiogenesis in cancer and other diseases. Nature. 2000; 407:249–257. [PubMed: 11001068]

Clasper S, Royston D, Baban D, Cao Y, Ewers S, Butz S, Vestweber D, Jackson DG. A novel gene expression profile in lymphatics associated with tumor growth and nodal metastasis. Cancer Res. 2008; 68:7293–7303. [PubMed: 18794116]

Coultas L, Chawengsaksophak K, Rossant J. Endothelial cells and VEGF in vascular development. Nature. 2005; 438:937–945. [PubMed: 16355211]

Dejana E, Lampugnani MG, Martinez-Estrada O, Bazzoni G. The molecular organization of endothelial junctions and their functional role in vascular morphogenesis and permeability. Int. J. Dev. Biol. 2000; 44:743–748. [PubMed: 11061439]

Ferrara N, Kerbel RS. Angiogenesis as a therapeutic target. Nature. 2005; 438:932–936. [PubMed: 16355210]

Folkman J. Angiogenesis in cancer, vascular rheumatoid and other disease. Nat. Med. 1995; 1:27–31. [PubMed: 7584949]

Gho YS, Kleinman HK, Sosne G. Angiogenic activity of human soluble intercellular adhesion molecule-1. Cancer Res. 1999; 59:5128–5132. [PubMed: 10537287]

Gupta GP, Nguyen DX, Chiang AC, Bos PD, Kim JY, Nadal C, Gomis RR, Manova-Todorova K, Massagué J. Mediators of vascular remodelling co-opted for sequential steps in lung metastasis. Nature. 2007; 446:765–770. [PubMed: 17429393]

Hara T, Ishida T, Cangara HM, Hirata K. Endothelial cell-selective adhesion molecule regulates albuminuria in diabetic nephropaty. Microvasc. Res. 2009; 77:348–355. [PubMed: 19323980]

Herard AL, Pierrot D, Hinrnrasky J, Kaplan H, Sheppard D, Puchelle E, Zahm JM. Fibronectin and its $\alpha_5\beta_1$-integrin receptor are involved in the wound-repair process of airway epithelium. Am. J. Physiol. Lung Cell Mol. Physiol. 1996; 271:726–733.

Hirata K, Ishida T, Penta K, Rezaee M, Yang E, Wohlgemuth J, Quertermous T. Cloning of an immunoglobulin family adhesion molecule selectively expressed by endothelial cells. J. Biol. Chem. 2001; 276:16223–16231. [PubMed: 11279107]

Ishida T, Kundu RK, Yang E, Hirata K, Ho YD, Quertermous T. Targeted distruption of endothelial cell-selective adhesion molecule inhibits angiogenic processes in vitro and in vivo. J. Biol. Chem. 2003; 278:34598–34604. [PubMed: 12819200]

Iñiguez MA, Rodríguez A, Volpert OV, Fresno M, Redondo JM. Cyclooxygenase-2: a therapeutic target in angiogenesis. Trends Mol. Med. 2003; 9:73–78. [PubMed: 12615041]

Kerbel RS. Tumor angiogenesis. N. Engl. J. 2008; 358:2039–2048.

Kimura R, Ishida T, Kuriyama M, Hirata K, Hayashi Y. Interaction of endothelial cell-selective adhesion molecule and MAGI-1 promotes mature cell-cell adhesion via activation of RhoA. Genes Cells. 2010; 15:385–396. [PubMed: 20298433]

Miles FL, Pruitt FL, Van Golen KL, Cooper CR. Stepping out of the flow : capillary extravasation in cancer metastasis. Clin. Exp. Metastasis. 2008; 25:305–324. [PubMed: 17906932]

Mihich E, Croce CM. Ninth annual Pezcoller Symposium: the biology of tumors. Cancer Res. 1999; 59:491–497. [PubMed: 9927068]

Nasdala I, Wolburg-Buchholz K, Wolburg H, Kuhn A, Ebnet K, Brachtendorf G, Samulowitz U, Kuster B, Engelhardt B, Vestweber D, Butz S. A transmembrane tight junction protein selectively expressed on endothelial cells and platelets. J. Biol. Chem. 2002; 277:16294–16303. [PubMed: 11847224]

Orrington-Myers J, Gao X, Kouklis P, Broman M, Rahman A, Vogel SM, Malik AB. Regulation of lung neutrophil recruitment by VE-cadherin. Am. J. Physiol. Lung Cell Mol. Physiol. 2006; 291:764–771.

Risau W. Mechanisms of angiogenesis. Nature. 1997; 386:671–674. [PubMed: 9109485]

Sökmen S, Sarioglu S, Füzün M, Terzi C, Küpelioglu A, Aslan B. Prognostic significance of angiogenesis in rectal cancer: a morphometric inverstigation. Anticancer Res. 2001; 21:4341–4348. [PubMed: 11908689]

Takatani T, Takahashi K, Uozumi Y, Shikata E, Yamamoto Y, Ito T, Matsuda T, Schaffer SW, Fujio Y, Azuma J. Taurine inhibits apoptosis by preventing formation of the Apaf-1/caspase-9 apoptosome. Am. J. Physiol. Cell Physiol. 2004; 287:949–953.

Talks KL, Harris HL. Current status of antiangiogenic factors. Br. J. Haematol. 2000; 109:477–489. [PubMed: 10886192]

Vestweber D. Molecular mechanisms that control endothelial cell contacts. J. Pathol. 2000; 190:281–291. [PubMed: 10685062]

Wegmann F, Ebnet K, Du Pasquier L, Vestweber D, Butz S. Endothelial adhesion molecule ESAM binds directly to the multidomain adaptor MAGI-1 and recruits it to cell contacts. Exp. Cell Res. 2004; 300:121–133. [PubMed: 15383320]

Wegmann F, Petri B, Khandoga AG, Moser C, Khandoga A, Volkery S, Li H, Nasdala I, Brandau O, Fäsler R, Butz S, Krombach F, Vestweber D. ESAM supports neutrofil extravasation, activation of Rho, and VEGF-induced vascular permeability. J. Exp. Med. 2006; 203:1671–1677. [PubMed: 16818677]

Yoder MC, Mead LE, Prater D, Krier TR, Mroueh KN, Li F, Krasich R, Temm CJ, Prchal JT, Ingram DA. Redefining endothelial progenitor cells via clonal analysis and hematopoietic stem/progenitor cell principals. Blood. 2007; 109:1801–1809. [PubMed: 17053059]

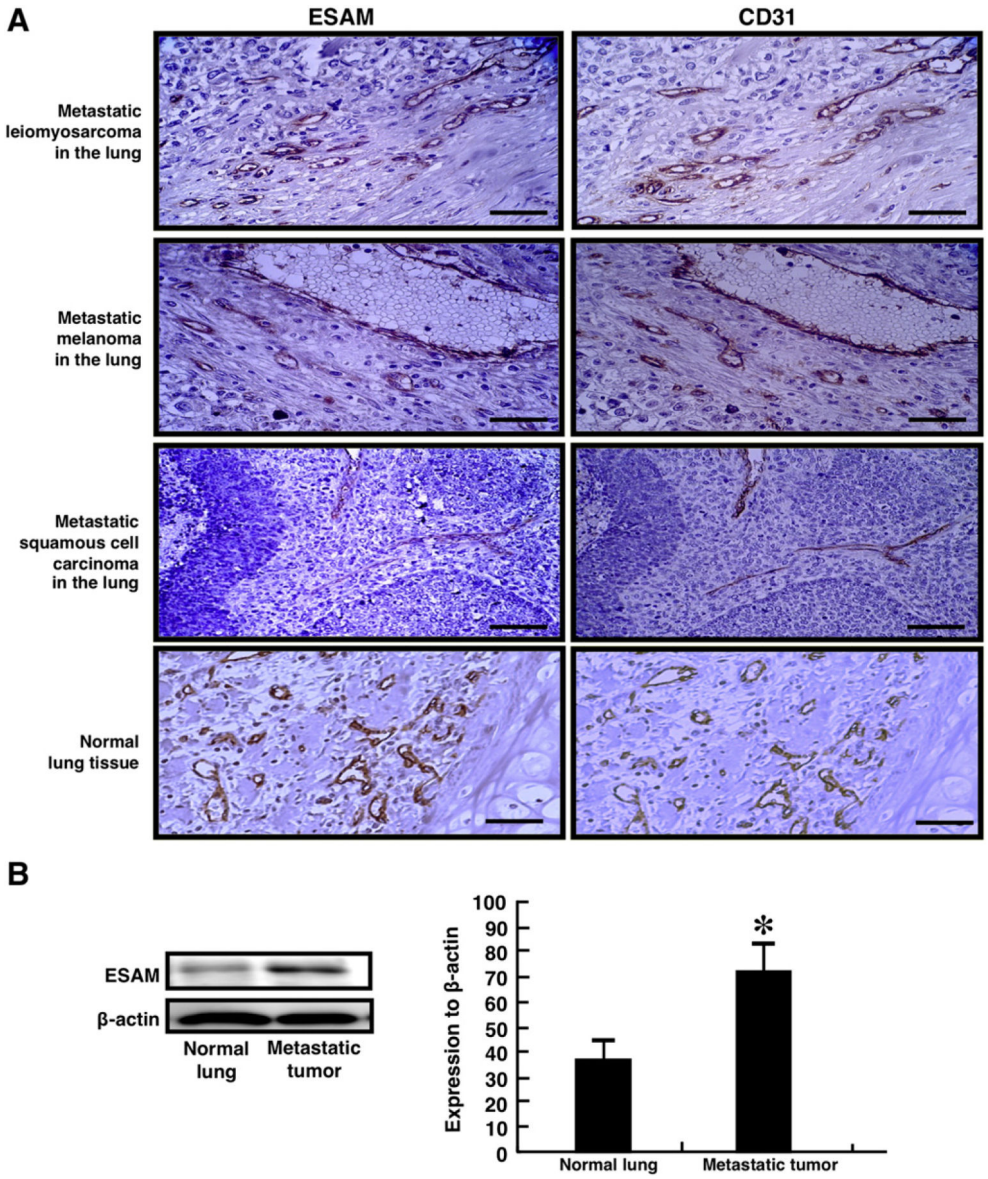


**Fig. 1.**

*ESAM* expression is increased in human metastatic tumors. (A) Immunohistochemical examination for ESAM and CD31 expressions in human metastatic tumor tissues. ESAM was present in the endothelium of human metastatic tumors and co-localized with CD31. The bar represents 200 μm. (B) Western blotting demonstrated that ESAM expression was higher in the whole tissue of human metastatic lung adenocarcinoma than in normal lung tissues (**P*<0.0001 vs. normal lungs).

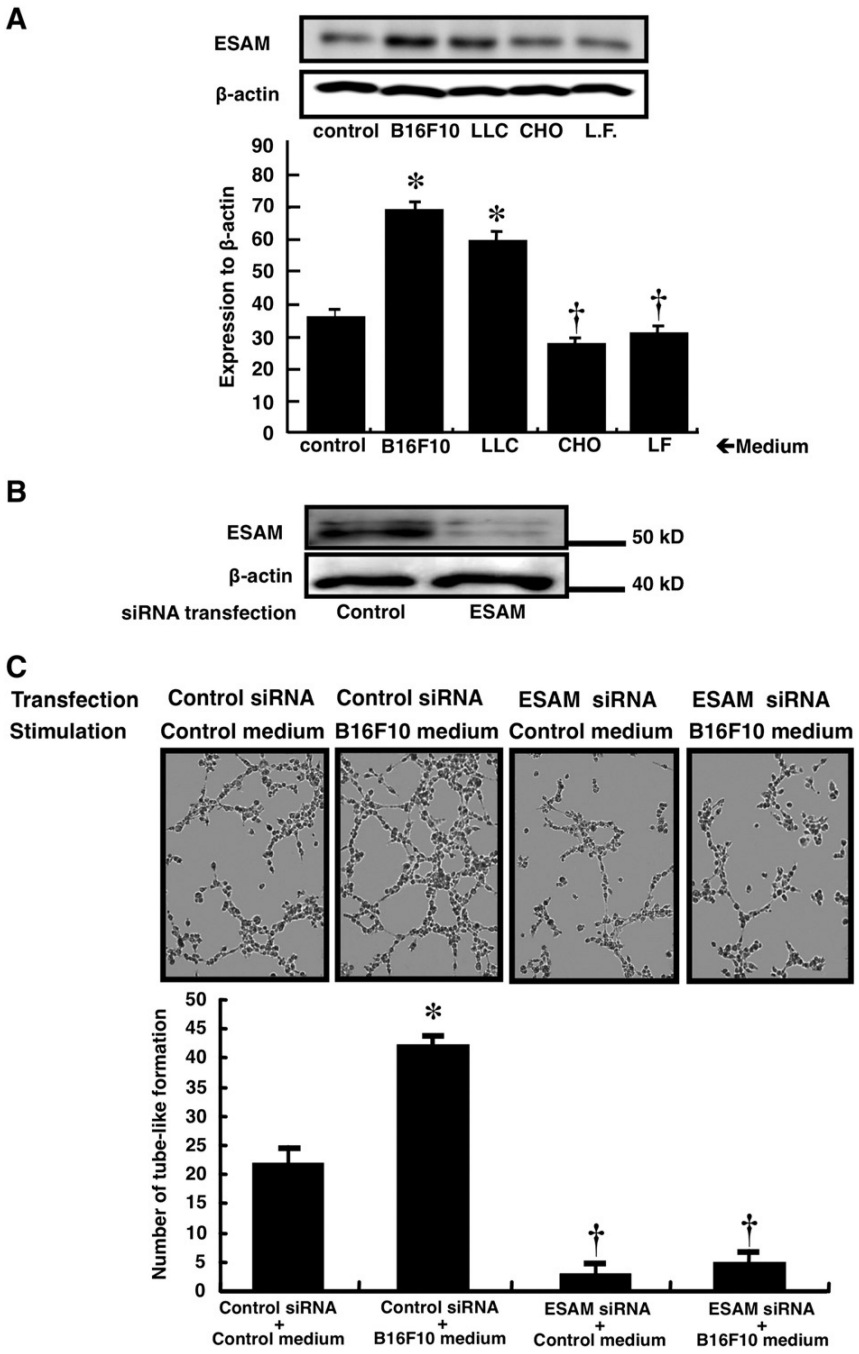


**Fig. 2.**

Cancer medium promotes tube formation through upregulation of *ESAM*. (A) Human endothelial EA.hy926 cells were stimulated with either a cancer medium (LLC and B16F10) or a non-cancer medium (CHO and LF). Western blotting revealed that the ESAM level was increased in response to the cancer medium while the non-cancer medium did not affect ESAM expression (*$P$<0.01 vs. control medium, †$P$<0.01 vs. cancer medium; $n$=6). (B) EA.hy926 cells were transfected with control- or *ESAM*-siRNA, and Western blotting confirmed the ESAM depletion. (C) *ESAM* downregulation attenuated the B16F10 cancer

medium-induced tube-like network formation. The graph shows a significant decrease in the number of tubes in *ESAM*-downregulated cells in response to control and B16F10 medium (*$P$<0.0001 vs. control siRNA + control medium, †$P$<0.0001 vs. corresponding control siRNA treatment; $n$=8).

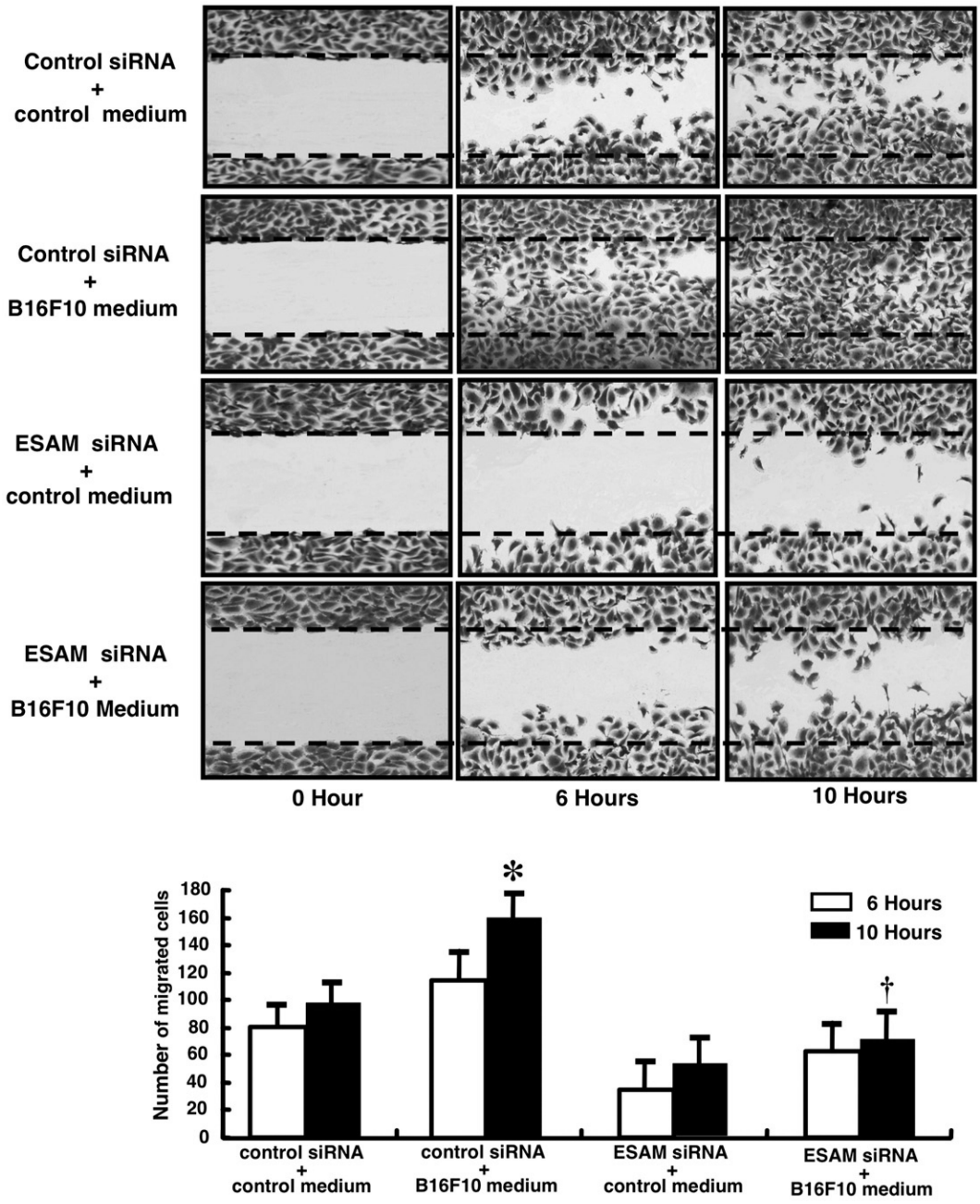


**Fig. 3.**

Effect *ESAM* on endothelial migration. The EA.hy926 cells were transfected with control- or *ESAM*-siRNA, and then used for a wound healing migration assay in response to B16F10 medium. Cell migration was inhibited by transfection of *ESAM*-siRNA (**P*<0.0001 vs. control siRNA + control medium, †*P*<0.0001 vs. control siRNA + B16F10 medium; *n*=8).

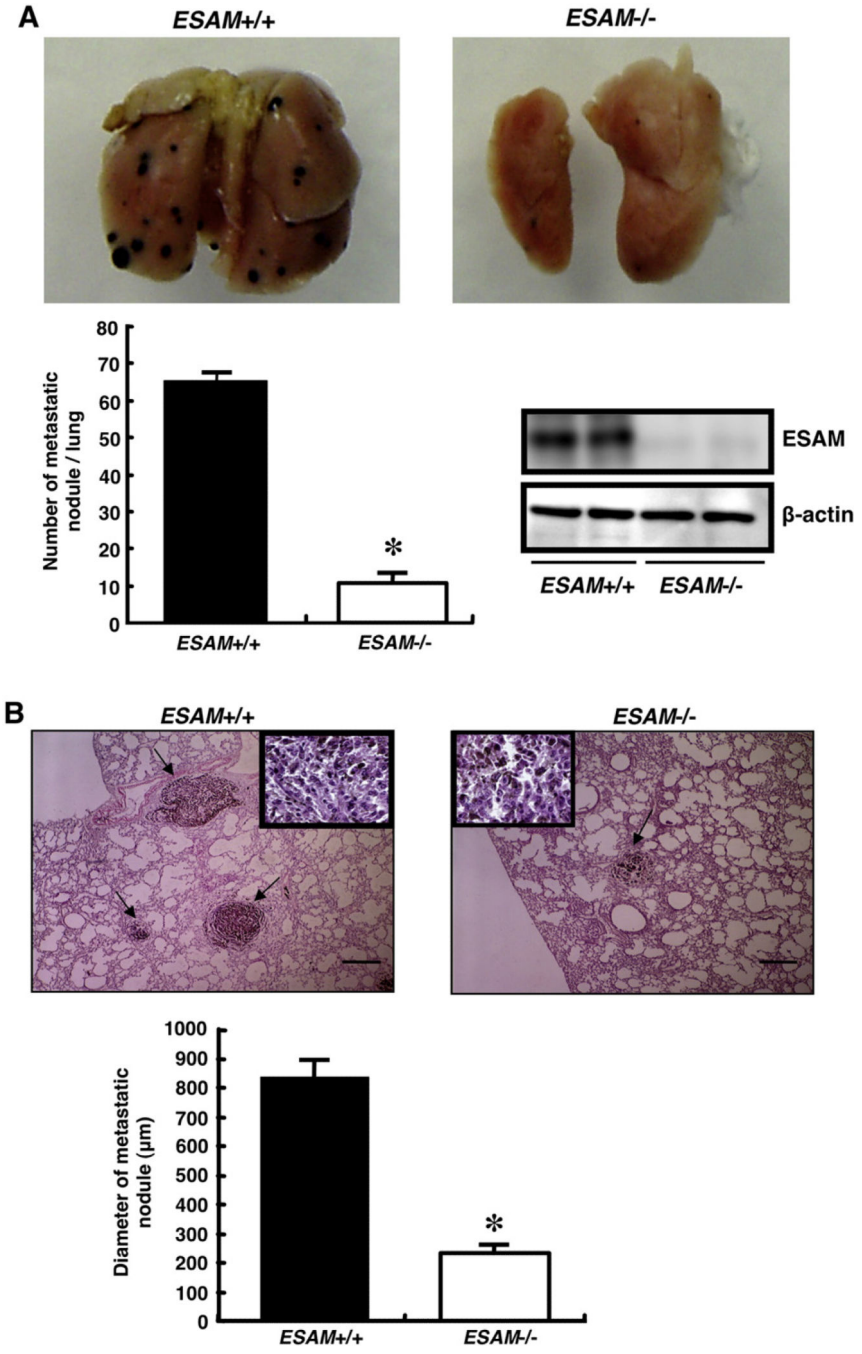


**Fig. 4.**

Reduced hematogeneous metastasis in the lung of *ESAM*−/− mice. B16F10 melanoma cells were injected into *ESAM*+/+ and *ESAM*−/− mice via the tail vein to generate a hematogeneous metastatic model. (A) Representative images of the lung (top panels). *ESAM*−/− mice had significantly fewer metastatic nodules than did *ESAM*+/+ mice (**P*<0.0001 vs. *ESAM*+/+; *n*=8, bottom left). ESAM was not detected in the lung of *ESAM* −/− mice (bottom right). (B) Histological analysis (H&E staining, ×100) revealed that the diameter of metastatic nodules in *ESAM*−/− was significantly smaller than that in *ESAM*+/+

mice (*$P$<0.0001 vs. *ESAM*+/+; $n$=8). Arrows indicate metastatic nodules in the lung. High magnification (×400) shows melanin pigments in melanoma cells. The bar represents 200 μm.

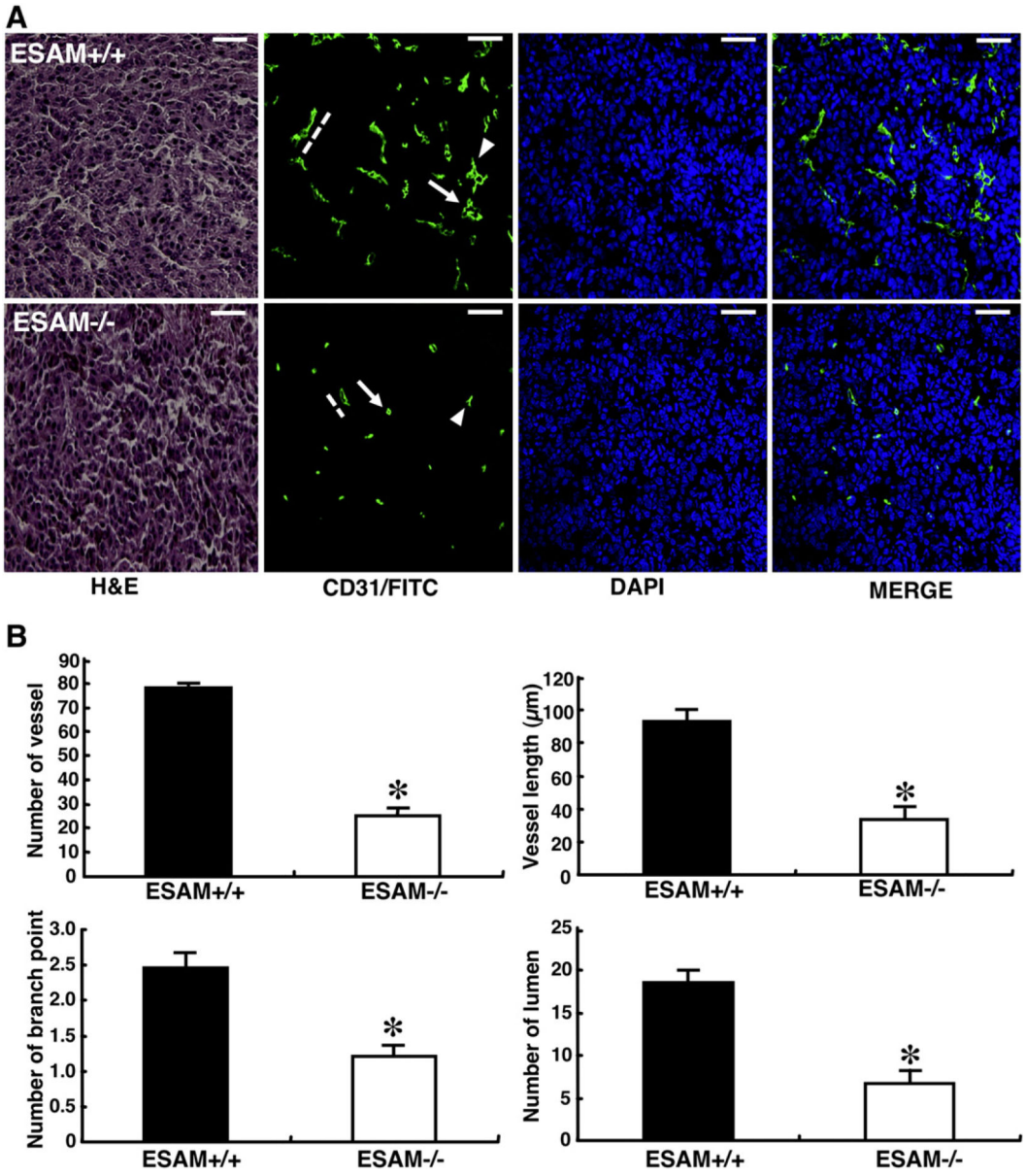


**Fig. 5.**

Attenuated angiogenesis in metastatic nodules of *ESAM*−/− mice. Vascular structures inside lung metastasis nodules from *ESAM*+/+ and *ESAM*−/− mice were stained with anti-CD31 (green) and DAPI (blue) for nuclear labeling (×200). (A) The total number of vascular structures was lower in *ESAM*−/− than in *ESAM*+/+ mice. *ESAM*−/− mice also featured morphological defects in the tumor vasculature such as in length (broken line), number of lumens (arrows) and extent of branching (arrow heads) when compared with *ESAM*+/+ mice. (B) These graphs show the average number and length of vessels, the number of lumens and the extent of branching of vessels. It is clear that *ESAM*−/− had fewer vascular structures and also had morphological defects in the vasculature (**P*<0.0001 vs. *ESAM*+/+; *n*=8). The bar represents 50 μm.

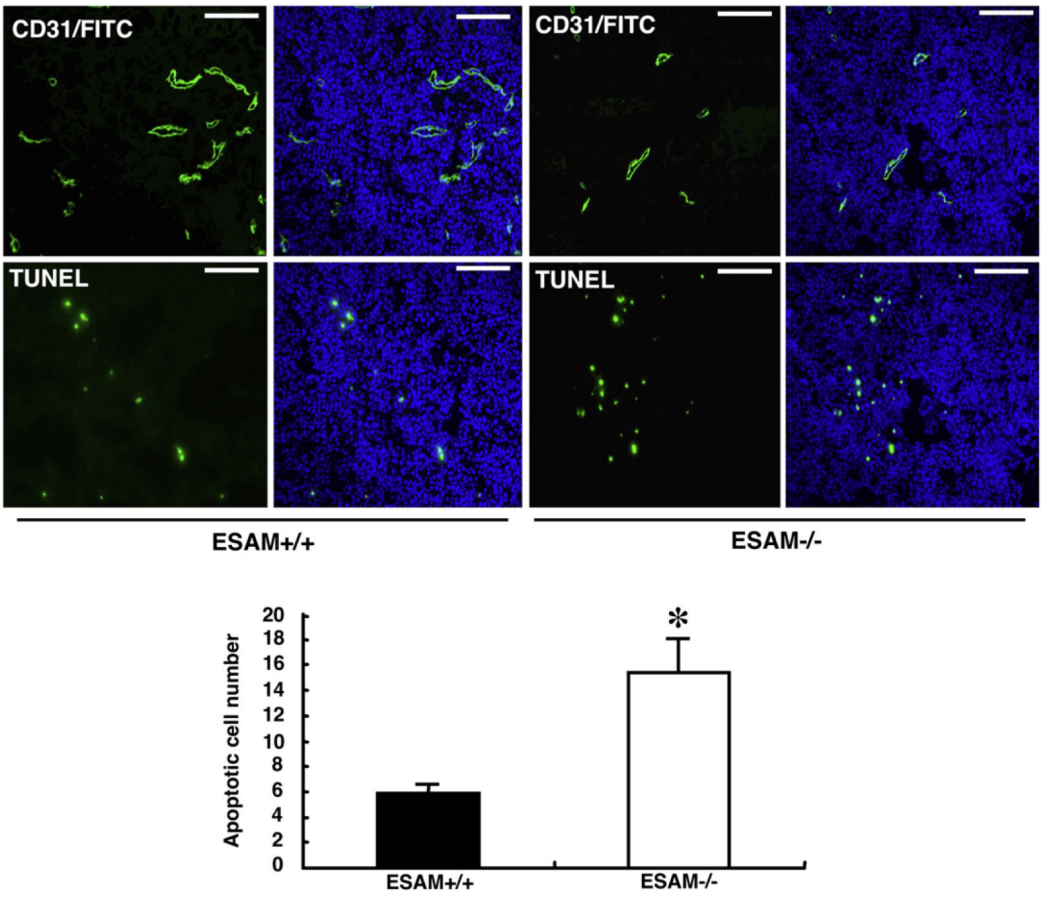


**Fig. 6.**

Reduced vascularity associated with tumor cell apoptosis in *ESAM*−/− mice. Sections of the lung metastatic nodules were stained for CD31 (vascular structure), TUNEL (apoptotic cells), or DAPI (nuclear staining). The total number of TUNEL-positive apoptotic cells was counted in 50 areas per section and the average number of apoptotic cells was higher in *ESAM*−/− mice (**P*<0.0001 vs. *ESAM*+/+; *n*=8). The bar represents 50 μm.